







## Article

# Supercritical CO<sub>2</sub> Extraction of Natural Compounds from Capuchin (*Tropaeolum majus*) Leaves and Seeds

Gabriel Corrêa <sup>1</sup>, Michel Rubens dos Reis Souza <sup>2</sup>, Eduardo Soares Nascimento <sup>3</sup>, Thiago Rodrigues Bjerck <sup>2</sup> , José Eduardo Gonçalves <sup>4</sup> , Cristiane Mengue Feniman Moritz <sup>5</sup> , Otávio Akira Sakai <sup>6</sup> , Erivaldo Antônio da Silva <sup>3</sup>, Renivaldo José dos Santos <sup>7</sup> , Edson Antônio da Silva <sup>8</sup>, Lucio Cardozo-Filho <sup>9</sup>, Andreia Fatima Zanette <sup>1</sup> and Leandro Ferreira-Pinto <sup>1,\*</sup> 

<sup>1</sup> Department of Engineering, School of Engineering and Sciences, São Paulo State University (UNESP), Rosana 19274-000, SP, Brazil; gabriel.correa02@unesp.br (G.C.)

<sup>2</sup> Institute of Technology and Research (ITP), Aracaju 49032-490, SE, Brazil; michel\_rubens@hotmail.com (M.R.d.R.S.); thiagobjerck@gmail.com (T.R.B.)

<sup>3</sup> Department of Cartography, School of Science and Technology, São Paulo State University (UNESP), Presidente Prudente 19060-900, SP, Brazil; eduardo.nascimento@unesp.br (E.S.N.); erivaldo.silva@unesp.br (E.A.d.S.)

<sup>4</sup> Programa de Pós-Graduação em Tecnologias Limpas, Universidade Cesumar e Instituto Cesumar de Ciência, Tecnologia e Inovação (ICETI), Maringá 87050-390, PR, Brazil; jose.goncalves@unicesumar.edu.br

<sup>5</sup> State University of Maringá, Umuarama Regional Campus, Umuarama 87506-370, PR, Brazil; crisfeniman@yahoo.com.br

<sup>6</sup> Federal Institute of Paraná (IFPR), Umuarama 87507-014, PR, Brazil; otavio.sakai@ifpr.edu.br

<sup>7</sup> Postgraduate Program in Science and Technology of Materials (POSMAT), School of Engineering and Sciences, São Paulo State University (UNESP), Rosana 19274-000, SP, Brazil

<sup>8</sup> Centro de Engenharias e Ciências Exatas, Universidade Estadual do Oeste do Paraná, Toledo 85903-000, PR, Brazil

<sup>9</sup> Programa de Pós-Graduação em Engenharia Química, Universidade Estadual de Maringá, Maringá 87020-900, PR, Brazil

\* Correspondence: leandro.f.pinto@unesp.br; Tel.: +55-18-32849683



**Citation:** Corrêa, G.; Souza, M.R.d.R.; Nascimento, E.S.; Rodrigues Bjerck, T.; Gonçalves, J.E.; Moritz, C.M.F.; Sakai, O.A.; Silva, E.A.d.; Santos, R.J.d.; da Silva, E.A.; et al. Supercritical CO<sub>2</sub> Extraction of Natural Compounds from Capuchin (*Tropaeolum majus*) Leaves and Seeds. *Processes* **2024**, *12*, 1566. <https://doi.org/10.3390/pr12081566>

Academic Editors: Philippe Evon and Evelien Uitterhaegen

Received: 13 June 2024

Revised: 18 July 2024

Accepted: 19 July 2024

Published: 26 July 2024

**Abstract:** This study investigated the supercritical CO<sub>2</sub> extraction of oils from capuchin (*Tropaeolum majus*) seeds (4.34% moisture content) and leaves (5.26% moisture content) and analyzed the effects of varying temperature and pressure conditions. The extraction yields were 3% for the seeds and 2% for the leaves. The seed extracts were rich in oleic, linoleic, and palmitic fatty acids, whereas the leaf extracts contained a high concentration of octacosanol (73.37%). Kinetic analysis revealed distinct mass transfer mechanisms during extraction, and the Sovová model effectively described the extraction kinetics, showing good agreement with experimental data (ADD% < 4%). An analysis of variance (ANOVA) demonstrated the impact of temperature and pressure on the yields, with temperature being the most influential factor. The experimental conditions ranged from 22 to 28 MPa and from 313.15 to 333.15 K. This study contributes to the understanding of capuchin oil extraction and its potential applications in various fields, owing to the presence of bioactive compounds.

**Keywords:** capuchin; supercritical extraction; CO<sub>2</sub>; oleic acid; octacosanol



**Copyright:** © 2024 by the authors. Licensee MDPI, Basel, Switzerland. This article is an open access article distributed under the terms and conditions of the Creative Commons Attribution (CC BY) license (<https://creativecommons.org/licenses/by/4.0/>).

## 1. Introduction

In recent years, there has been a growing interest in exploring natural resources for their diverse applications in nutrition, health, and industry. Among these resources, capuchin (*Tropaeolum majus*) has emerged as a subject of intense scientific inquiry due to its versatility. Capuchin is known in South America for its culinary and traditional medicinal properties. However, its potential extends far beyond these uses, prompting researchers to focus on its chemical composition and extraction processes [1,2].

Originating from Brazil, Mexico, and Peru, *Tropaeolum majus*, commonly known in Brazil as “capuchin”, “chaguinha”, and “nasturtium”, is a herbaceous plant with striking

flowers, which can be either simple or double. The plant is approximately 2–3 m long and 30–40 cm high [1]. It is an important medicinal, ornamental, and edible plant [2]. This species contains a variety of bioactive compounds, including flavonoids, carotenoids, and other polyphenols, which are known for their anti-inflammatory activities [3].

Preclinical studies on *Tropaeolum majus* have shown antibacterial action in the urinary tract, diuretic effects without renal calcium loss, hypotensive and cardiorenal protective effects, and antifungal and antiviral properties. These properties make it useful for treating bronchitis, acute sinusitis, and flu, owing to its high vitamin content [4,5]. Empirically, *Tropaeolum majus* is believed to support emotional energy, addressing manifestations of distress, frustration, anxiety, and depression [6]. This plant has recently gained popularity as an antidepressant [7].

Furthermore, *Tropaeolum majus* contains volatile oils, flavonoids, glucosinolates, and other bioactive compounds [8,9]. Volatile oils are secondary metabolites in plants that are rich in terpenoids and phenolic compounds, such as carvacrol and thymol, whose antimicrobial properties are influenced by their hydrophobicity and the presence of hydroxyl groups [10]. Additionally, *Tropaeolum majus* contains aliphatic acids, such as octacosanol, nonacosanol, nonacosanediol, lutein, provitamin A, and  $\beta$ -carotene in its flowers and leaves [11]. Octacosanol, a long-chain fatty alcohol, has neuroprotective effects and may enhance physical performance [12].

Capuchin presents an intriguing opportunity for the extraction of its active constituents. The most frequently used method for extracting capuchin is solvent extraction. Supercritical fluid extraction, particularly that using carbon dioxide (CO<sub>2</sub>) as a solvent, has become increasingly popular for extracting bioactive compounds from various plant sources [13,14]. The use of carbon dioxide (CO<sub>2</sub>) eliminates the need for extensive heating during the extraction of thermolabile chemicals. Understanding the intricacies of this extraction process, including the influence of parameters such as temperature and pressure, is essential for maximizing the yield and quality [15,16].

Pressurized/supercritical gas technology offers higher yields than other techniques owing to the intrinsic characteristics of supercritical fluid extraction, such as the enhanced transport and diffusion of supercritical or near-supercritical gasses into the matrix during the extraction process. Temperature and pressure control can also be used to extract bioactive components from oleaginous matrices. In addition to the substantially higher yield, another advantage of supercritical extraction is the absence of residual organic solvents [17,18].

This study investigated the influence of temperature and pressure on the extraction of seed and leaf extracts from capuchin. Supercritical CO<sub>2</sub> is used to improve the total yield and fatty acid profile and to increase the content of bioactive compounds. A second-order quadratic model was used to calculate the mass transfer and characterize the observed kinetic curves.

## 2. Experimental

### 2.1. Sample Preparation

Plant matrices, capuchin leaves, and seeds were collected from the Pontal do Paranapanema region of Brazil. The plant matrices were dried in a ventilated oven at 333.15 K for 48 h until they reached a constant mass [19,20], ground using a domestic blender, and sieved through W.S. Tyler sieves (Mentor, OH, USA). The dried leaves and seeds were ground, and a particle size of 0.85 mm (20 mesh) was selected for screening samples. Subsequently, samples were vacuum-packed in polyethylene bags and frozen. Particle density ( $\rho_t$ ) was determined using a helium gas pycnometer Ultrapyc 1200e (Quantachrome Instruments, Boynton Beach, FL, USA)

### 2.2. Supercritical CO<sub>2</sub> Extraction

The experiments were conducted using a CO<sub>2</sub> cylinder, two thermostatically regulated baths, an Isco 500 D syringe pump, a jacketed extraction vessel (1.91 cm in diameter

and 16.8 cm in height), and an absolute pressure transducer (Smar LD301, Sertãozinho, SP, Brazil) (See Figure 1). Further details regarding the instruments and experimental procedures can be found in previous studies [21–23].

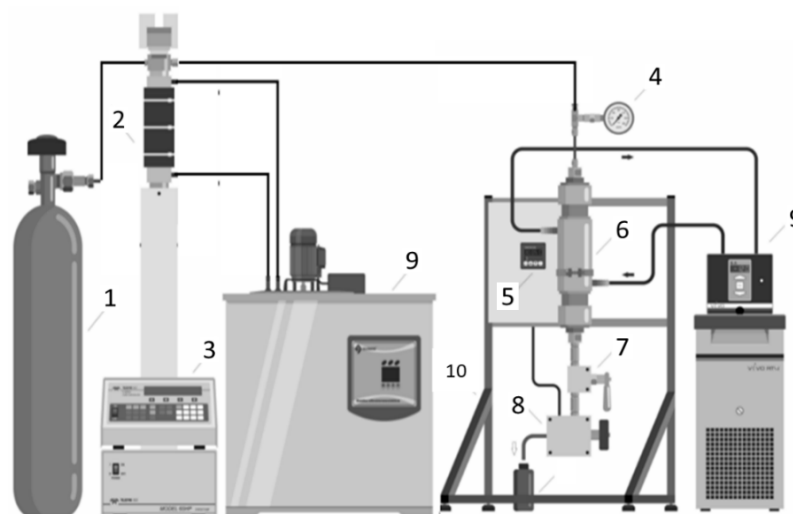


**Figure 1.** Schematic of the experimental supercritical extraction unit: 1—CO<sub>2</sub> cylinder; 2—syringe pump; 3—thermostatic bath; 4—pressure indicator; 5—temperature controller/indicator; 6—extractor; 7—valve; 8—needle-type valve attached to an aluminum jacket for heating; 9—thermostatic bath; 10—aluminum structure.

The moisture content after drying was 5.26% and 4.34% for the leaves and seeds, respectively. The extraction vessel was loaded with 0.01 kg of dried capuchin leaves and seeds and the remaining space in the extraction cell was filled with inert glass spheres. This configuration ensures that CO<sub>2</sub> passes through the fixed bed upon delivery to the extractor before reaching the ground seed. The syringe pump and extractor were simultaneously pressurized at the designated extraction temperatures. After attaining the desired working pressure, the system was allowed to cool for 30 min to equilibrium, ensuring that the solvent was fully saturated before commencing the extraction process.

Extractions were carried out at pressures of 22, 25, and 28 MPa and temperatures of 313.15 K, 323.15 K, and 333.15 K, with a constant CO<sub>2</sub> flow rate of 2.0 mL·min<sup>-1</sup>. The experimental design followed a 2<sup>2</sup> factorial procedure with triplicate runs at the central point (Table 1). The CO<sub>2</sub> flow rate was precisely controlled at 2.0 mL·min<sup>-1</sup> using a micrometer valve (Parker Autoclave Engineers, Erie, PA, USA) and maintained at 353.15 K. The extract was collected in glass bottles and weighed during six initial cycles of 5 min and six–nine cycles of 10 min each. The extraction yield was determined gravimetrically using an analytical balance and was calculated as the ratio of the total mass extracted to the initial mass of the leaves in the extractor (on a dry basis).

**Table 1.** Two-level factorial design.

Factors	Symbols	Units	Levels		
			−1	0	+1
Temperature	T	K	313.15	323.15	333.15
Pressure	P	MPa	22	25	28

### 2.3. Oil Characterization

The extract samples were weighed on an analytical balance, diluted in dichloromethane (n = 3) to a concentration of 1000 µg mL<sup>-1</sup>, and then injected into the established chromatographic method.

For the one-dimensional Gas Chromatography Mass Spectrometry (GC-MS) chromatographic analyses, a Shimadzu gas chromatograph coupled to a mass spectrometer (model GCMS-QP2010 plus, Kyoto, Japan) equipped with an automatic injector AOC-20i auto sampler/auto injector (Shimadzu, Kyoto, Japan) and a DB-5MS capillary column (50 m; 0.25 mm internal diameter and 0.25  $\mu\text{m}$  stationary phase thickness) was used. The temperature program started at 313.15 K, with a heating rate of 2 K  $\text{min}^{-1}$  up to 473.15 K, followed by an increase of 10 K  $\text{min}^{-1}$  up to 573.15 K (held for 15 min). The injector, interface, and ionization source temperatures were 523.15 K, 573.15 K, and 553.15 K, respectively. The helium gas flow rate (99.999%) was 0.8 mL  $\text{min}^{-1}$ . A 1  $\mu\text{L}$  injection (1000  $\mu\text{g mL}^{-1}$ ) was performed in split mode at 1:50. Data were collected using the GCMS Postrun Analysis program (Shimadzu), which includes databases for the NIST14.lb and NIST14.lbs spectral libraries.

#### 2.4. Statistical Analysis

The data were subjected to an analysis of variance (ANOVA) at 5% significance, followed by the Tukey test using Statistica Software version 8.0 [24]. The main effects and interactions were computed using Design Expert software version 12 [25], which evaluates the main effects and interactions and determines the influence of the independent factors on the response.

#### 2.5. Kinetics of the Extraction—Model of the Sovová

The Sovová model [26] considers two mass-transfer stages and three distinct extraction periods. First period: Easy-to-access oil extraction. This stage depends on the solubility in the fluid phase and is characterized by a linear curve with a slope close to the oil solubility value in the solvent. Second period: decreasing the extraction rate, followed by the extraction of hard-to-access oil, controlled by an internal diffusion mechanism. Third period: the extraction curve becomes almost linear with a much lower extraction rate than that in the first period.

The Sovová Model Equations (1)–(7) are as follows:

First period ( $t < t_{\text{CER}}$ ): the constant extraction rate is calculated as follows:

$$X(t) = \frac{\dot{m}_F Y_S t}{m_S X_0} [1 - \exp(-Z)] \quad (1)$$

Second period ( $t_{\text{CER}} \leq t \leq t_{\text{FER}}$ ): the decreasing rate is calculated as follows:

$$X(t) = \frac{\dot{m}_F Y_S}{m_S X_0} \left[ t - t_{\text{CER}} \exp\left(\frac{Z Y_S}{W X_0} \ln\left\{\frac{1}{1-r} \left(\exp\left(\frac{W \dot{m}_F}{m_s}\right)(t - t_{\text{CER}}) - r\right)\right\} - Z\right) \right] \quad (2)$$

Third period ( $t > t_{\text{FER}}$ ): the diffusion-controlled extraction rate is calculated as follows:

$$X(t) = \frac{1}{X_0} \left[ X_0 - \frac{Y_S}{W} \ln\left\{1 + \left(\exp\left(\frac{W X_0}{Y_S}\right) - 1\right) \exp\left(\frac{W \dot{m}_F (t_{\text{CER}} - t)}{m_s}\right) r\right\} \right] \quad (3)$$

where

$$Z = \frac{k_F a m_s \rho_F}{\dot{m}_F \rho_S (1 - \varepsilon)} \quad (4)$$

$$W = \frac{m_s k_s a}{\dot{m}_F (1 - \varepsilon)} \quad (5)$$

$$t_{\text{CER}} = \frac{(1-r)m_s X_0}{Y_S \dot{m}_F} \quad (6)$$

$$t_{\text{FER}} = t_{\text{CER}} + \frac{m_s}{W \dot{m}_F} \ln\left[r + (1-r) \exp\left(\frac{W X_0}{Y_S}\right)\right] \quad (7)$$

where

$\dot{m}_F$  is the solvent mass flow rate ( $\text{g}\cdot\text{min}^{-1}$ );  $Y_s$  is the apparent oil solubility in the solvent ( $\text{g}_{\text{oil}}\cdot\text{g}_{\text{solvent}}^{-1}$ );  $t$  is the extraction time (min);  $X_0$  is the initial oil concentration in the solid matrix ( $\text{g}_{\text{oil}}\cdot\text{g}_{\text{solvent}}^{-1}$ );  $m_s$  is the mass of non-extractable material (g);  $r$  is the fraction of easily accessible oil;  $t_{\text{CER}}$  is the end of the first extraction period (min);  $t_{\text{FER}}$  is the end of the second extraction period (min);  $k_{\text{Fa}}$  is the mass transfer coefficient of the fluid phase ( $\text{min}^{-1}$ );  $k_{\text{sa}}$  is the mass transfer coefficient of the solid phase ( $\text{min}^{-1}$ );  $\varepsilon$  is the porosity of the extraction bed;  $\rho_F$  is the density of the fluid ( $\text{g}\cdot\text{cm}^{-3}$ ); and  $\rho_s$  is the solid density ( $\text{g}\cdot\text{cm}^{-3}$ ).

The parameter ( $r$ ) in the Sovová model is related to the fraction of hard-to-access solutes within the solid. The parameters  $Z$ ,  $W$ , and  $r$  were calculated using the downhill simplex method, which minimizes the objective function given by Equation (8), as follows:

$$F = \sum_{i=1}^{n_{\text{exp}}} \sum_{j=1}^N \left( m_{\text{oil},j}^{\text{Calc}} - m_{\text{oil},j}^{\text{Exp}} \right)^2 \quad (8)$$

where  $m_{\text{oil},j}^{\text{Calc}}$  is the calculated mass of oil extracted using the Sovová model;  $m_{\text{oil},j}^{\text{Exp}}$  is the experimentally obtained oil mass; and  $n_{\text{exp}}$  is the number of extractions.

This model provides a comprehensive framework for describing the supercritical  $\text{CO}_2$  extraction process and can be used to optimize the extraction conditions for various plant materials.

### 3. Results and Discussions

#### 3.1. Extraction Yield

The experimental conditions and total yields of capuchin seed and leaf oils extracted using supercritical  $\text{CO}_2$  are listed in Table 2. The highest extraction yield was 2.1 wt% for capuchin leaves and 3.0 wt% for capuchin seeds.

**Table 2.** Experimental conditions and extraction yield for capuchin seed and leaf oil extraction using supercritical  $\text{CO}_2$ .

Run	Temperature (K)	Pressure (MPa)	Yield (wt%)
Capuchin Leaves			
1	313.15	22	0.98
2	333.15	22	1.64
3	313.15	28	1.05
4	333.15	28	2.10
5	318.15	25	1.51
6	318.15	25	1.39
7	318.15	25	1.48
Capuchin Seeds			
1	313.15	22	2.97
2	333.15	22	2.42
3	313.15	28	3.00
4	333.15	28	2.29
5	318.15	25	2.74
6	318.15	25	2.75
7	318.15	25	2.75

The capuchin leaves had lower extract quantities. In other words, the yields from this matrix were lower than those obtained from capuchin seed extracts. Generally, the results obtained from the leaf extraction were below 2%. Seed extraction was superior to that obtained from the leaves, reaching a value of 3%. This yield was expected, given that the quantity of oil was predominant in the seeds. Musolino et al. [27] reported extraction yields from capuchin leaves, obtaining 1.3% for n-hexane, 0.9% for dichloromethane, and

0.9% for ethyl acetate. Thus, when comparing the data obtained in this study with the data from the literature, a convergent agreement between the results is observed.

Most extracts were removed from the plant matrices within the first 20 min. After this period, the amount of the extracted material decreased significantly. By analyzing Figures 2–5, changes in the slopes of the extraction kinetic curves were observed. These changes in pitch occur due to variations in convective and diffusive mass transfer mechanisms. The speed of the mass transfer process was influenced more by the convective mechanism in the fluid phase and less by the diffusive mechanism. A discontinuity effect in the surface layer was initiated with the gradual removal of the lipid material. At the beginning of this discontinuity, there was a decrease in the extraction rate governed by the diffusion mechanism.

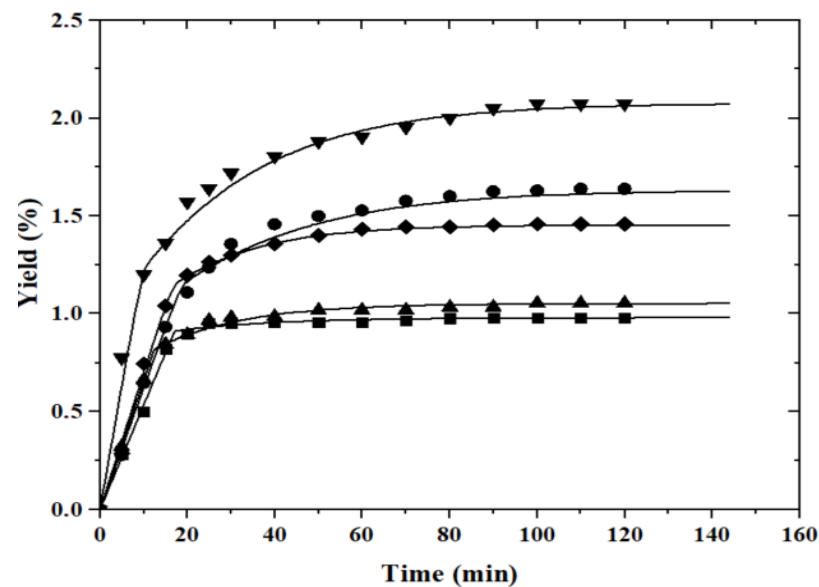


**Figure 2.** Experimental kinetic curves extraction with supercritical CO<sub>2</sub> fitted using Sovová model (—) of capuchin leaves: 313.15 K (■, 22 MPa; ▲, 28 MPa); 323.15 K (◆, 25 MPa); 333.15 K (●, 22 MPa; ▼, 28 MPa) with a constant flow rate of 2.0 mL·min<sup>-1</sup>.

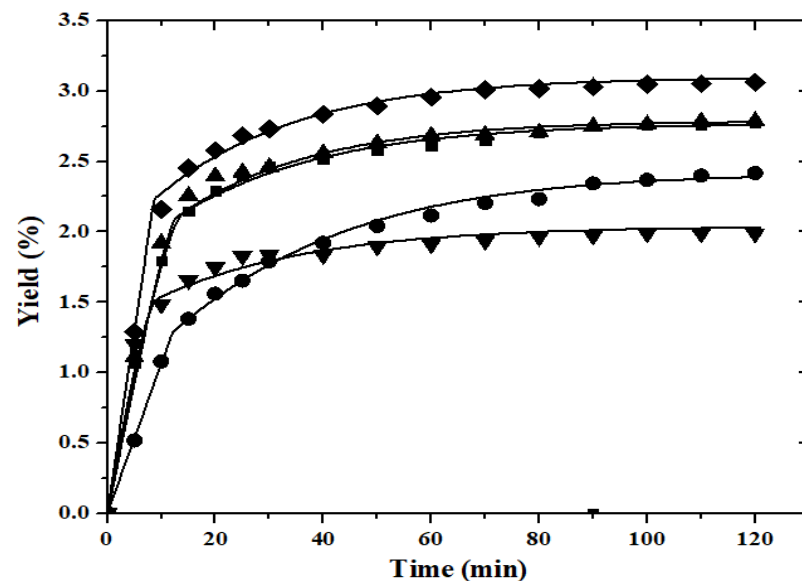


**Figure 3.** Experimental kinetic curves extraction with supercritical CO<sub>2</sub> fitted using Sovová model (—) of capuchin seeds: 313.15 K (■, 22 MPa; ▲, 28 MPa); 323.15 K (◆, 25 MPa); 333.15 K (●, 22 MPa; ▼, 28 MPa) with a constant flow rate of 2.0 mL·min<sup>-1</sup>.



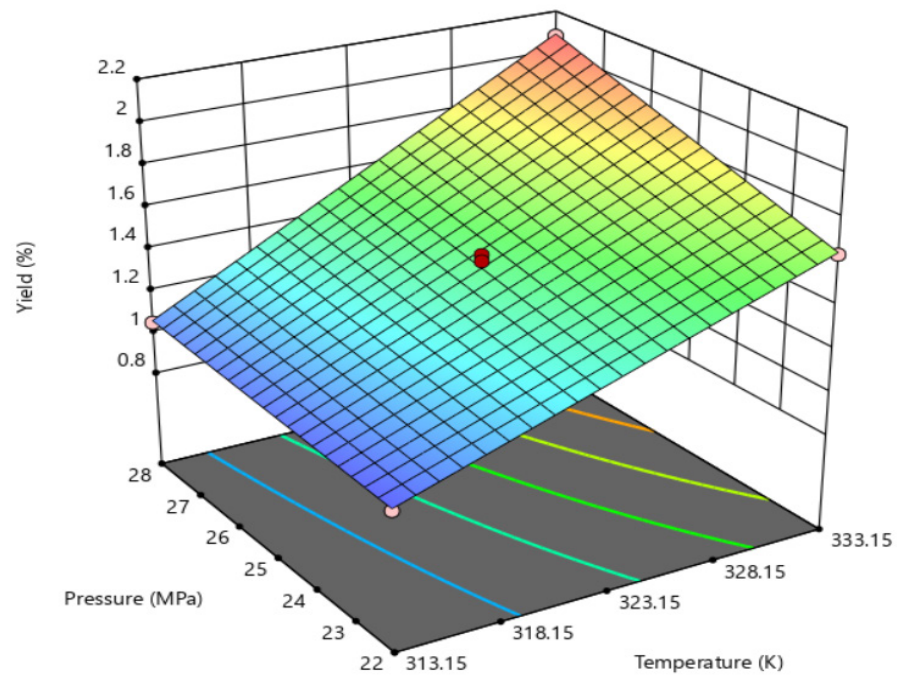


**Figure 4.** The response surface refers to the extraction yield of capuchin leaves as a function of temperature and pressure, at a constant flow rate of  $2.0 \text{ mL}\cdot\text{min}^{-1}$ .

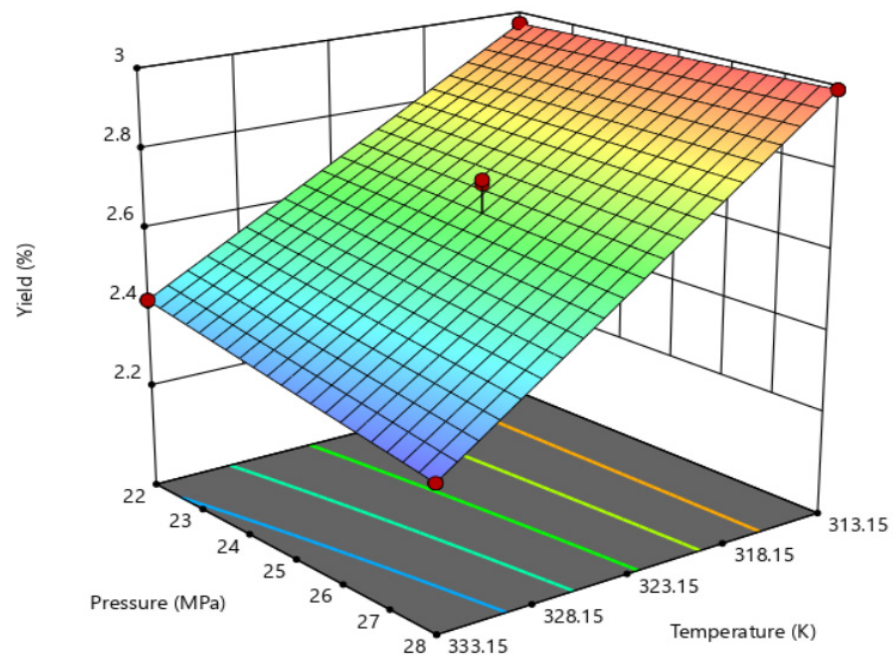


**Figure 5.** The response surface refers to the oil extraction yield of capuchin seeds as a function of temperature and pressure at a constant flow rate of  $2.0 \text{ mL}\cdot\text{min}^{-1}$ .

The influence of pressure and temperature on the extraction yield can be visualized using response surface graphs, as shown in Figure 4 (leaves) and Figure 5 (seeds).

For capuchin leaves, temperature plays a primary role, whereas pressure acts as a supporting factor influencing the extraction yield. The highest extraction yields were achieved at a temperature of 333.15 K.

For the extraction of oil from capuchin seeds, a different behavior was observed compared to the leaf extraction. The increase in yield from 303.15 K to 333.15 K was

relatively small, suggesting that the additional energy cost at higher temperatures may not justify potential increases in extraction gains.

By analyzing the differences in yield behavior for the two plant matrices, when observing the effects of pressure and temperature, it is possible to suggest that, owing to the greater availability of extract (oil) in capuchin seeds, the application of the lower proposed conditions (313.15 K and 22 MPa) was sufficient to carry almost all the extracts. Thus, increasing the temperature and pressure during the extraction process did not significantly improve the extraction percentage. In contrast, for capuchin leaves, which have a lower amount of extractable material, an increase in temperature combined with an increase in pressure provided the best extraction yield. In other words, the two factors (pressure and temperature) acted synergistically. Because the leaves have less extractable material than the seeds, the influence of these factors at their higher levels (333.15 K and 28 MPa) provided a considerable increase in yield.

For both plant matrices, pressure was an important factor in achieving the best yields, indicating that higher CO<sub>2</sub> densities provided better oil extraction yields. However, for the extraction process with capuchin seeds, considering the adopted pressure range (between 22 and 28 MPa), the increase in pressure did not result in significant gains.

Pressure shortens the distance between the molecules and increases the interactions between CO<sub>2</sub> and the sample, which can promote convective mass transfer [28,29]. Shi et al. [30] showed that increasing the temperature and pressure helps to remove more complex extracts using supercritical CO<sub>2</sub> extraction. Similar results have been reported previously [31].

These results highlight the importance of adjusting the extraction parameters for specific plant materials. The differences observed under optimal conditions likely resulted from variations in the chemical composition and structure of the capuchin leaf and seed matrix. Optimizing the process parameters is crucial for maximizing efficiency and resource utilization.

Variations in yield were assessed using an analysis of variance (ANOVA) (Table 3). The analysis revealed a significant linear model for temperature and pressure factors (two-factor interaction) in each of the studied plant matrices.  $T$  denotes the temperature and  $P$  represents the pressure in these equations (Equations (9) and (10)). These variables are crucial in determining the study outcomes, showing an intricate relationship between extraction conditions and yield.

$$\text{Capuchin leaves yield} = 1.45 - 0.4225 T + 0.1275 P + 0.0925 T.P \quad (9)$$

$$\text{Capuchin seeds yield} = 2.70 - 0.3125 T - 0.0275 P + 0.0375 T.P \quad (10)$$

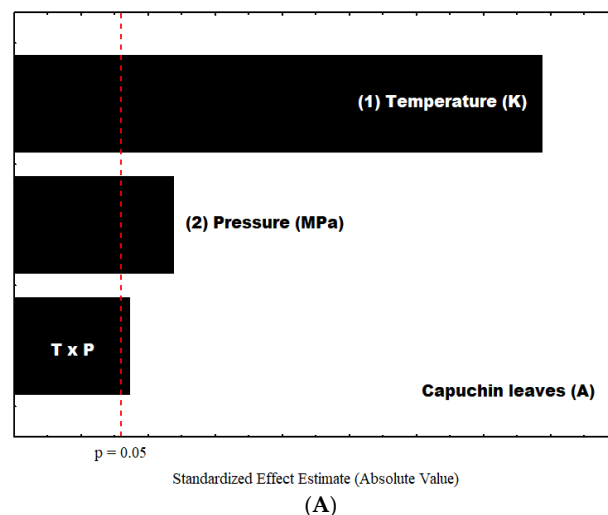
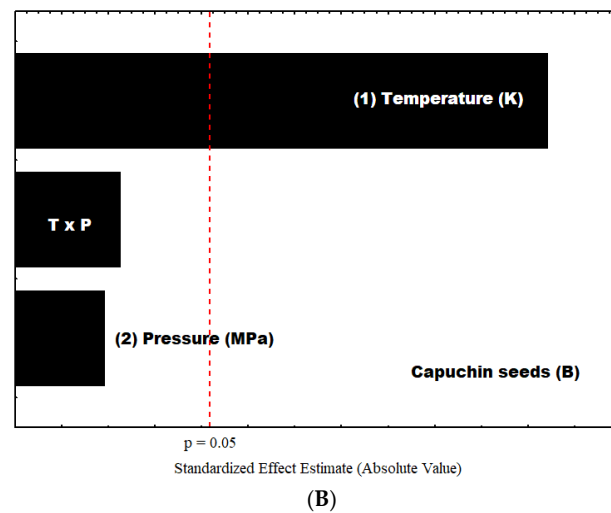


Figure 6. Cont.





**Figure 6.** Pareto chart: estimation of linear effects of variables. (A) Capuchin leaves and (B) capuchin seeds.

**Table 3.** Variance analysis data for the extracts were obtained using  $2^2$  factorial designs for the extraction from plant matrices with carbon dioxide.

Terms	Sum of Squares	Degrees of Freedom	Mean Squares	F-Value	<i>p</i> -Value	R <sup>2</sup>
Capuchin Leaves						
Model	0.8133	3	0.2711	69.51	0.0142	0.9895
T	0.7140	1	0.7140	183.08	0.0054	
P	0.0650	1	0.0650	16.67	0.0551	
T.P	0.0342	1	0.0342	8.78	0.0976	
Pure Error	0.0078	2	0.0039			
Cor Total	0.8219	6				
Capuchin Seeds						
Model	0.3993	3	0.1331	36.93	0.0072	0.9736
T	0.3906	1	0.3906	108.40	0.0019	
P	0.0030	1	0.0030	0.8394	0.4271	
T.P	0.0056	1	0.0056	1.56	0.3001	
Pure Error	0.0001	2	0.0107	322.32	0.0031	
Cor Total	0.4101	6				

T = Temperature; P = Pressure.

The analysis of variance (ANOVA) of the experimental results, as illustrated in the Pareto chart in Figure 6A,B, revealed that temperature (T) and pressure (P) significantly influenced yield (Y), with a *p*-value of less than 0.05.

### 3.2. Mathematic Modeling of the Extraction

The adjustable parameters for the Sovová model and the solubility of extracts from plant matrices in CO<sub>2</sub> were determined using the dynamic method and were calculated based on the slopes of the kinetic curves, as detailed in Table 4. The model conformed to the extraction kinetic curves, as indicated by the R<sup>2</sup> values shown in Figures 2 and 3.

**Table 4.** Experimental conditions, extraction yield results, and adjustment parameters of the mathematical model for the extraction of natural compounds using supercritical CO<sub>2</sub>.

Run	Z	W	r	S (g <sub>oil</sub> ·g <sub>solvent</sub> <sup>-1</sup> )	<i>t</i> <sub>CER</sub> (min)	<i>t</i> <sub>FER</sub> (min)	<i>K</i> <sub>Fa</sub> (min <sup>-1</sup> )	<i>K</i> <sub>Sa</sub> (min <sup>-1</sup> )	ADD (%)	R <sup>2</sup>
Capuchin Leaves										
1	81.45	0.06	0.098	0.001	0.20	17.27	5.86	0.009	1.59	0.994
2	14.11	0.04	0.387	0.001	1.14	19.87	1.48	0.007	2.69	0.993
3	84.10	0.05	0.299	0.001	0.13	12.58	8.82	0.011	1.16	0.994
4	7.59	0.04	0.469	0.001	1.14	11.04	0.79	0.008	4.02	0.956
5–7 *	11.46	0.05	0.300	0.001	1.27	17.88	1.20	0.011	1.60	0.997
Capuchin Seeds										
1	6.34	0.034	0.27	0.002	0.64	5.55	0.48	0.64	1.85	0.989
2	13.61	0.034	0.53	0.001	0.89	15.04	1.03	0.89	1.38	0.997
3	2.73	0.033	0.24	0.002	1.17	4.99	0.21	1.17	1.70	0.987
4	2.72	0.035	0.27	0.002	0.84	3.40	0.20	0.84	2.62	0.943
5–7 *	2.95	0.030	0.26	0.002	1.04	4.60	0.23	1.04	1.06	0.996

Note: extraction carried out in triplicate \*.

The change in the slope of the extraction kinetic curves occurred because of variations in the convective and diffusive mass-transfer mechanisms. The speed of the mass transfer process is primarily determined by the convection mechanism in the fluid phase. As the extract was gradually removed, a discontinuity effect was observed on the surface layer. At this point, a decreasing extraction rate was observed, initiating a diffusive process in which the oil that was initially difficult to access began to be extracted.

The mass transfer coefficients in the solvent phase (*K*<sub>Fa</sub>) were higher than those in *K*<sub>Sa</sub> (the solid phase), indicating that the easily accessible oil provided a higher extraction yield. The *K*<sub>Sa</sub> values were lower than the *K*<sub>Fa</sub> values, signifying more difficulties in the diffusion process and, consequently, in the solubilization of hard-to-reach oils, as confirmed by other researchers [14,29,32,33]. The *t*<sub>CER</sub> value indicates the moment at which the extraction of oil from inside the particles begins. In contrast, *t*<sub>FER</sub> values represent the extraction of easily accessible crude compounds.

where Z and W represent the dimensionless parameters in the Sovová model, S denotes the solubility, r is the mass of the easily accessible oil, *t*<sub>CER</sub> marks the point when oil extraction from inside the particles is initiated, and *t*<sub>FER</sub> indicates the moment when extraction from the easily accessible solute is complete. *K*<sub>Fa</sub> is the mass transfer coefficient of the solvent phase and *K*<sub>Sa</sub> is the mass transfer coefficient of the solid phase. R<sup>2</sup> denotes the coefficient of determination, which is a statistical measure that indicates how well the model fits data.

### 3.3. Extract Components

#### 3.3.1. Capuchin Seeds

A chemical analysis of capuchin seed oil (Table 5) was conducted for the experiment with the highest yield (T = 313.15 K and P = 28 MPa), revealing a complex composition, comprising significant proportions of oleic acid (22.50%), linoleic acid (19.74%), and palmitic acid (9.87%). These fatty acids play pivotal roles in human nutrition and health. Oleic acid, a monounsaturated omega-9 fatty acid, is associated with cardiovascular benefits and contributes to reduced LDL cholesterol levels. Linoleic acid, an essential polyunsaturated omega-6 fatty acid, maintains a healthy skin and cell membrane structure. Palmitic acid, a saturated fatty acid, is a natural component of various oils and fats and is essential for cell membrane stability.

**Table 5.** Chemical constituents of the capuchin seed oil.

Compound	Chemical Class	Peak Area (%)
Hexadecanoic acid	fatty acid	9.87 ± 0.01
Linoleic acid	fatty acid	19.74 ± 0.09
Oleic acid	fatty acid	22.50 ± 0.25
Tricosane	alkane	1.02 ± 0.11
Tetracosane	alkane	2.74 ± 0.13
Pentacosane	alkane	3.12 ± 0.06
Hexacosane	alkane	3.88 ± 0.04
Heptacosane	alkane	4.20 ± 0.08
Octacosane	alkane	3.24 ± 0.19
Unknown	-	24.78 ± 0.30
Nonacosane	alkane	2.89 ± 0.15
Triacosane	alkane	2.02 ± 0.15

Mean ± standard deviation (n = 3) \*

Additionally, alkanes were also present, including tricosane, tetracosane, pentacosane, hexacosane, heptacosane, octacosane, nonacosane, and triacosane. In smaller quantities, these alkanes are vital components of plant defense mechanisms. They create a protective layer on seed surfaces, prevent water loss, protect against pathogens, and mitigate environmental stresses.

An unidentified compound, constituting 24.78% of seed oil, adds to the complexity of its chemical composition and warrants further investigation. This unknown compound signifies the intricate nature of plant biochemistry and potentially holds significance for ecological adaptation and applications in various fields.

In summary, the substantial concentrations of oleic, linoleic, and palmitic acids underscored the nutritional value of capuchin seeds. Simultaneously, the diverse array of alkanes, along with unidentified compounds, highlights the intricate and multifaceted chemical profile of capuchin seed oil. These constituents contribute to the ecological resilience of plants and hold promise for potential applications in human nutrition, health, and industrial contexts, thereby meriting ongoing scientific exploration and study.

### 3.3.2. Capuchin Leaves

An analysis of the chemical constituents of the capuchin leaf extract, detailed in Table 6, was conducted for the experiment with the highest yield (T = 333.15 K and P = 28 MPa), which revealed notable components crucial to plant physiology and potential human applications. Nonacosane (17.68%) and octacosanol (73.37%) were the most common.

**Table 6.** Chemical constituents of the capuchin leaves extract.

Compound	Chemical Class	Peak Area (%)
Unknown	-	2.31
Hexadecanoic acid	fatty acid	2.80
Unknown	-	2.09
Oleic acid	alkane	1.75
Nonacosane	alkane	17.68
Octacosanol	alkane	73.37

Nonacosanes, alkanes identified in a sample, play a vital role in plant biology. Alkanes such as nonacosanes are integral components of the cuticular wax layer that covers plant surfaces. This wax layer acts as a protective barrier, preventing excessive water loss through transpiration and safeguarding the plant against various environmental stresses, including pathogens and UV radiation.

Octacosanol, another prominent constituent of capuchin leaves, is a long-chain fatty alcohol known for its potential health benefits. Studies have suggested that octacosanol

possesses antioxidant properties, which may contribute to improved exercise performance and endurance in animals. Additionally, octacosanol has been investigated for its neuroprotective effects and has shown promise in mitigating certain neurodegenerative conditions.

The presence of these compounds in capuchin leaves indicates the plant's adaptive mechanisms and ability to produce bioactive molecules with diverse applications. The role of nonacosane in cuticle formation emphasizes the resilience and ability of plants to thrive under various environmental conditions. Owing to its potential health benefits, octacosanol underscores the significance of plants in traditional medicine and as a potential source of natural products with therapeutic applications.

In summary, identifying nonacosane and octacosanol in capuchin leaves sheds light on the plant's ecological strategies and highlights their potential pharmacological and medicinal applications. These compounds serve as intriguing subjects for further research, both in understanding plant biology and exploring their applications in human health and wellness.

#### 4. Conclusions

This study investigated the extraction of oils from capuchin (*Tropaeolum majus*) seeds and leaves using supercritical CO<sub>2</sub>, and explored variations in temperature and pressure. The extraction yields were 3% for seeds and 2% for leaves, possibly because of the higher oil content of the seeds. The moisture content was determined to be 5.26% for the leaves and 4.34% for the seeds. The kinetic analysis highlighted the importance of the first 20 min of extraction, revealing distinct mass transfer mechanisms.

Chemical characterization of the extracts identified essential fatty acids such as oleic, linoleic, and palmitic acids, predominantly in the seeds, indicating their nutritional value. Additionally, some alkanes were detected, suggesting plant defense mechanisms. Nonacosane and octacosanol were found at higher concentrations in the leaves, with octacosanol representing 73.37% of the leaf extracts, potentially indicating neuroprotective properties.

The analysis of variance (ANOVA) demonstrated the impact of temperature and pressure on extraction yields, with elevated temperatures increasing leaf yields. The response surface methodology indicated the importance of these parameters, while the Pareto analysis showed that temperature was the most influential factor. The experimental conditions chosen for this study were a pressure range of 22 MPa to 28 MPa and a temperature range of 313.15 K to 333.15 K.

Mathematical modeling of the extraction kinetics using the Sovová model exhibited good agreement with the experimental data, validating the effectiveness of the model in representing the extraction processes. These models captured the complexities of the mass transfer mechanisms and proved useful in optimizing the extraction process.

In summary, this study contributes to the understanding of supercritical CO<sub>2</sub> extraction of capuchin oils, detailing the processes involved and the chemical composition of the plant. The results obtained may have applications in nutrition, health, and industry because of the rich composition of bioactive compounds in capuchin seeds and leaves.

**Author Contributions:** Conceptualization, L.F.-P., A.F.Z. and L.C.-F.; methodology, G.C., M.R.d.R.S., E.S.N., T.R.B., J.E.G., C.M.F.M. and O.A.S.; software, E.A.d.S. (Edson Antônio da Silva); formal analysis, L.F.-P., E.A.d.S. (Erivaldo Antônio da Silva) and R.J.d.S.; data curation, L.F.-P.; writing—original draft preparation, G.C. and L.F.-P.; writing—review and editing, L.F.-P.; visualization, L.F.-P. and A.F.Z. All authors have read and agreed to the published version of the manuscript.

**Funding:** This study was financed by the Fundação de Amparo à Pesquisa do Estado de São Paulo: Grant Number 2018/23063-1.

**Data Availability Statement:** The original contributions presented in the study are included in the article and further inquiries can be directed to the corresponding authors.

**Acknowledgments:** The authors would like to thank the Coordination for the Improvement of the Staff of Higher Education (CAPES/PNPD Process number: 88887.357888/2019-00). LF-P thanks the

financial support of the Fundação de Amparo à Pesquisa do Estado de São Paulo, FAPESP (Brazil), through the grant 2018/23063-1.

**Conflicts of Interest:** The authors declare no conflicts of interest.

## References

- Melo, A.C.; Costa, S.C.A.; Castro, A.F.; Souza, A.N.V.; Sato, S.W.; Lívero, F.A.R.; Lourenço, E.L.B.; Baretta, I.P.; Lovato, E.C.W. Hydroethanolic Extract of *Tropaeolum majus* Promotes Anxiolytic Effects on Rats. *Rev. Bras. Farmacogn.* **2018**, *28*, 589–593. [\[CrossRef\]](#)
- Ribeiro, W.S.; Barbosa, J.A.; Costa, L.C.; Bruno, R.L.A.; Almeida, E.I.B.; Silva, K.R.G.; Braga Júnior, J.M.; Bezerra, A.K.D. Conservação e Fisiologia Pós-Colheita de Folhas de Capuchinha (*Tropaeolum majus* L.). *Rev. Bras. Plantas Med.* **2011**, *13*, 598–605. [\[CrossRef\]](#)
- Butnariu, M.; Bostan, C. Antimicrobial and Anti-Inflammatory Activities of the Volatile Oil Compounds from *Tropaeolum majus* L. (Nasturtium). *Afr. J. Biotechnol.* **2011**, *10*, 5900–5909. [\[CrossRef\]](#)
- Barboza, L.N.; Prando, T.B.L.; Dalsenter, P.R.; Gasparotto, F.M.; Gasparotto, F.; Jacomassi, E.; Araújo, V.D.O.; Lourenço, E.L.B.; Gasparotto Junior, A. Prolonged Diuretic Activity and Calcium-Sparing Effect of *Tropaeolum majus*: Evidence in the Prevention of Osteoporosis. *Evid. Based Complement. Altern. Med.* **2014**, *2014*, 958291. [\[CrossRef\]](#) [\[PubMed\]](#)
- Conrad, A.; Kolberg, T.; Engels, I.; Frank, U. In-Vitro-Untersuchungen Zur Antibakteriellen Wirksamkeit Einer Kombination Aus Kapuzinerkressenkraut (*Tropaeoli majoris* Herba) Und Meerrettichwurzel (*Armoraciae rusticanae* Radix). *Arzneimittelforschung* **2011**, *56*, 842–849. [\[CrossRef\]](#)
- Campos, A.C.; Fogaca, M.V.; Aguiar, D.C.; Guimaraes, F.S. Animal Models of Anxiety Disorders and Stress. *Rev. Bras. Psiquiatr.* **2013**, *35*, S101–S111. [\[CrossRef\]](#) [\[PubMed\]](#)
- da Silva, I.C.M.; dos Santos, W.L.; Leal, I.C.R.; Maria das Graças, B.Z.; Feirhmann, A.C.; Cabral, V.F.; Macedo, E.N.; Cardozo-Filho, L. Extraction of Essential Oil from *Cyperus articulatus* L. Var. *Articulatus* (Pripricoa) with Pressurized CO<sub>2</sub>. *J. Supercrit. Fluids* **2014**, *88*, 134–141. [\[CrossRef\]](#)
- Jakubczyk, K.; Janda, K.; Watychowicz, K.; Łukasiak, J.; Wolska, J. Garden Nasturtium (*Tropaeolum majus* L.)—A Source of Mineral Elements and Bioactive Compounds. *Rocz. Panstw. Zakl. Hig.* **2018**, *69*, 119–126.
- Vrca, I.; Ramić, D.; Fredotović, Ž.; Smole Možina, S.; Blažević, I.; Bilušić, T. Chemical Composition and Biological Activity of Essential Oil and Extract from the Seeds of *Tropaeolum majus* L. Var. *Altum*. *Food Technol. Biotechnol.* **2022**, *60*, 533–542. [\[CrossRef\]](#)
- Junior, A.G.; Prando, T.B.L.; Gebara, K.S.; Gasparotto, F.M.; dos Reis Lívero, F.A.; de Lima, D.P.; da Silva Gomes, R.; Lourenço, E.L.B. Protective Cardiorenal Effects of *Tropaeolum majus* L. In Rats With Renovascular Hypertension. *J. Young Pharm.* **2017**, *9*, 251–257. [\[CrossRef\]](#)
- Frei, P.; Nadegger, C.; Vollmar, A.M.; Müller, T.; Moser, S. Structural Characterization, and Antioxidative and Anti-Inflammatory Activities of Phylloxanthobilins in *Tropaeolum majus*, a Plant with Relevance in Phytomedicine. *Planta Med.* **2024**, *90*, 641–650. [\[CrossRef\]](#) [\[PubMed\]](#)
- Teixeira, F.S.; Costa, P.T.; Soares, A.M.S.; Fontes, A.L.; Pintado, M.E.; Vidigal, S.S.M.P.; Pimentel, L.L.; Rodríguez-Alcalá, L.M. Novel Lipids to Regulate Obesity and Brain Function: Comparing Available Evidence and Insights from QSAR In Silico Models. *Foods* **2023**, *12*, 2576. [\[CrossRef\]](#)
- Botelho, J.R.S.; Medeiros, N.G.; Rodrigues, A.M.C.; Araújo, M.E.; Machado, N.T.; Guimarães Santos, A.; Santos, I.R.; Gomes-Leal, W.; Carvalho, R.N. Black Sesame (*Sesamum indicum* L.) Seeds Extracts by CO<sub>2</sub> Supercritical Fluid Extraction: Isotherms of Global Yield, Kinetics Data, Total Fatty Acids, Phytosterols and Neuroprotective Effects. *J. Supercrit. Fluids* **2014**, *93*, 49–55. [\[CrossRef\]](#)
- Pedersetti, M.M.; Palú, F.; da Silva, E.A.; Rohling, J.H.; Cardozo-Filho, L.; Dariva, C. Extraction of Canola Seed (*Brassica napus*) Oil Using Compressed Propane and Supercritical Carbon Dioxide. *J. Food Eng.* **2011**, *102*, 189–196. [\[CrossRef\]](#)
- McHugh, M.; Krukonis, V. *Supercritical Fluid Extraction: Principles and Practice*; Elsevier: Amsterdam, The Netherlands, 2013; ISBN 9780080518176.
- Zougagh, M.; Valcárcel, M.; Ríos, A. Supercritical Fluid Extraction: A Critical Review of Its Analytical Usefulness. *TrAC Trends Anal. Chem.* **2004**, *23*, 399–405. [\[CrossRef\]](#)
- Sihvonen, M. Advances in Supercritical Carbon Dioxide Technologies. *Trends Food Sci. Technol.* **1999**, *10*, 217–222. [\[CrossRef\]](#)
- Lima, J.C.; de Araújo, P.C.C.; dos Santos Croscato, G.; de Almeida, O.; Cabral, V.F.; Ferreira-Pinto, L.; Cardozo-Filho, L. Experimental Phase Equilibrium Data for Rotenone in Supercritical Carbon Dioxide. *J. Chem. Eng. Data* **2019**, *64*, 2357–2362. [\[CrossRef\]](#)
- Nurhaslina, C.R.; Andi Bacho, S.; Mustapa, A.N. Review on Drying Methods for Herbal Plants. *Mater. Today Proc.* **2022**, *63*, S122–S139. [\[CrossRef\]](#)
- Freschet, G.T.; Pagès, L.; Iversen, C.M.; Comas, L.H.; Rewald, B.; Roumet, C.; Klimešová, J.; Zadworny, M.; Poorter, H.; Postma, J.A.; et al. A Starting Guide to Root Ecology: Strengthening Ecological Concepts and Standardising Root Classification, Sampling, Processing and Trait Measurements. *New Phytol.* **2021**, *232*, 973–1122. [\[CrossRef\]](#)
- Garcia, V.A.D.S.; Cabral, V.F.; Zanoelo, É.F.; da Silva, C.; Filho, L.C. Extraction of Mucuna Seed Oil Using Supercritical Carbon Dioxide to Increase the Concentration of L-Dopa in the Defatted Meal. *J. Supercrit. Fluids* **2012**, *69*, 75–81. [\[CrossRef\]](#)

22. Gonçalves, R.M.; Lemos, C.O.T.; Leal, I.C.R.; Nakamura, C.V.; Cortez, D.A.G.; da Silva, E.A.; Cabral, V.F.; Cardozo-Filho, L. Comparing Conventional and Supercritical Extraction of (-)-Mammea A/BB and the Antioxidant Activity of Calophyllum Brasiliense Extracts. *Molecules* **2013**, *18*, 6215–6229. [[CrossRef](#)] [[PubMed](#)]
23. Silva, M.O.; Camacho, F.P.; Ferreira-Pinto, L.; Giufrida, W.M.; Vieira, A.M.S.; Visentaine, J.V.; Vedoy, D.R.L.; Cardozo-Filho, L. Extraction and Phase Behaviour of Moringa Oleifera Seed Oil Using Compressed Propane. *Can. J. Chem. Eng.* **2016**, *94*, 2195–2201. [[CrossRef](#)]
24. Weiß, C.H. StatSoft, Inc., Tulsa, OK.: STATISTICA, Version 8. *ASTA Adv. Stat. Anal.* **2007**, *91*, 339–341. [[CrossRef](#)]
25. Anderson, M.J.; Whitcomb, P.J. Design of Experiments. In *Kirk-Othmer Encyclopedia of Chemical Technology*; Wiley: Hoboken, NJ, USA, 2010; pp. 1–22.
26. Sovová, H. Rate of the Vegetable Oil Extraction with Supercritical CO<sub>2</sub>—I. Modelling of Extraction Curves. *Chem. Eng. Sci.* **1994**, *49*, 409–414. [[CrossRef](#)]
27. Musolino, V.; Marrelli, M.; Perri, M.R.; Palermo, M.; Gliozzi, M.; Mollace, V.; Conforti, F. *Centranthus ruber* (L.) DC. and *Tropaeolum majus* L.: Phytochemical Profile, In Vitro Anti-Denaturation Effects and Lipase Inhibitory Activity of Two Ornamental Plants Traditionally Used as Herbal Remedies. *Molecules* **2022**, *28*, 32. [[CrossRef](#)] [[PubMed](#)]
28. Wang, X.; Wang, C.; Zha, X.; Mei, Y.; Xia, J.; Jiao, Z. Supercritical Carbon Dioxide Extraction of  $\beta$ -Carotene and  $\alpha$ -Tocopherol from Pumpkin: A Box–Behnken Design for Extraction Variables. *Anal. Methods* **2017**, *9*, 294–303. [[CrossRef](#)]
29. Mateus, L.S.; Dutra, J.M.; Favareto, R.; da Silva, E.A.; Ferreira Pinto, L.; da Silva, C.; Cardozo-Filho, L. Optimization Studies and Compositional Oil Analysis of Pequi (*Caryocar brasiliense* Cambess) Almonds by Supercritical CO<sub>2</sub> Extraction. *Molecules* **2023**, *28*, 1030. [[CrossRef](#)] [[PubMed](#)]
30. Shi, J.; Yi, C.; Ye, X.; Xue, S.; Jiang, Y.; Ma, Y.; Liu, D. Effects of Supercritical CO<sub>2</sub> Fluid Parameters on Chemical Composition and Yield of Carotenoids Extracted from Pumpkin. *LWT Food Sci. Technol.* **2010**, *43*, 39–44. [[CrossRef](#)]
31. Frohlich, P.C.; Santos, K.A.; Palú, F.; Cardozo-Filho, L.; da Silva, C.; da Silva, E.A. Evaluation of the Effects of Temperature and Pressure on the Extraction of Eugenol from Clove (*Syzygium aromaticum*) Leaves Using Supercritical CO<sub>2</sub>. *J. Supercrit. Fluids* **2019**, *143*, 313–320. [[CrossRef](#)]
32. Wenceslau, B.R.; Santos, K.A.; da Silva, E.A.; Cardozo-Filho, L.; da Silva, C.; Favareto, R. Guariroba (*Syagrus oleracea*) Kernel Oil Extraction Using Supercritical CO<sub>2</sub> and Compressed Propane and Its Characterization. *J. Supercrit. Fluids* **2021**, *177*, 105326. [[CrossRef](#)]
33. Klein, E.J.; Johann, G.; da Silva, E.A.; Vieira, M.G.A. Mathematical Modeling of Supercritical CO<sub>2</sub> Extraction of Eugenia Pyriformis Cambess. Leaves. *Chem. Eng. Commun.* **2021**, *208*, 1543–1552. [[CrossRef](#)]

**Disclaimer/Publisher’s Note:** The statements, opinions and data contained in all publications are solely those of the individual author(s) and contributor(s) and not of MDPI and/or the editor(s). MDPI and/or the editor(s) disclaim responsibility for any injury to people or property resulting from any ideas, methods, instructions or products referred to in the content.